



Comparative investigation of reactivity of different kinds of fly ash in alkaline media

Iwona Wilińska¹ · Barbara Pacewska¹

Received: 10 September 2018 / Accepted: 26 April 2019 / Published online: 16 May 2019
© The Author(s) 2019

Abstract

Comparison of the influence of temperature and different alkali activators on the reactivity of two types of fly ash (conventional, fluidized) was presented. The main emphasis was put on fluidized fly ash as potential component of binding mixtures containing low amount of cement. Conventional fly ash was used as a reference. It was found that for these materials the key differences affecting products of activation are: availability of calcium and sulfate ions as well as structure of fly ash grains influencing dissolution of aluminate and silicate species. Fluidized fly ash, contrary to conventional fly ash, undergoes reaction in 0.1 M solutions of hydroxides forming mainly ettringite. In the case of 4 M hydroxides, both fly ashes undergo hydration processes. Conventional fly ash formed mainly amorphous aluminosilicate gel, while fluidized fly ash may create zeolitic products especially in the case of elevated temperature of early hydration. Sulfate and alkali ions can be incorporated into aluminosilicate structure of new formed products; however, this process depends strictly on the type of used hydroxide and its concentration. The presence of $\text{Ca}(\text{OH})_2$, carbonates and alkali sulfates was also registered in the case of hydrated fluidized fly ash.

Keywords Fly ash · Activation · Hydration · Thermal analysis · Infrared spectroscopy

Introduction

Fly ash has been utilized as supplementary cementitious material for decades. Different amounts of this by-product in cement composite can be considered: up to 35 mass% (typical amount), about 50% (high volume fly ash concretes (HVFAC) [1–5]) or even 70–80% (very HVFAC [6–10]). Moreover, there is also possibility of using fly ash as binding material performed without cement (alkali activated fly ash, geopolymers) [11–18].

Geopolymers are composed of aluminosilicates of framework consisting of tetrahedral coordination of Si^{4+} and Al^{3+} [11–14, 19, 20]. The negative charges in the three-dimensional aluminosilicate structure are compensated by alkali cations [15–17, 21]. Despite that the processes of alkali activation of aluminosilicate source

materials have been studied for years, their mechanism is not fully understood [17]. In general, formation of geopolymer consists of sequences of dissolution, polymerization, polycondensation and precipitation processes, while dissolution of aluminosilicate source material at early reaction period plays a crucial role. For such transformations, starting aluminosilicate material needs strong alkaline medium and it also often requires elevated temperature. Some researchers pointed out that the presence of calcium components (introduced, e.g., with slag or small amount of cement) in the starting material causes that the development of suitable properties of the final material may be obtained without heat treatment [22, 23].

It should be noted that not only fly ash but also other aluminosilicate materials [11, 12, 14, 17, 24], such as different types of slags [25, 26] or metakaolin [26–30], can be applied as starting materials for geopolymers. However, fly ashes from different sources [26, 31, 32], mixtures made of different fly ashes [33] or compositions of fly ash and other materials [34] still arouse interest.

Despite the unabated interest in geopolymers, a new type of binder, which may be classified between high

✉ Iwona Wilińska
Iwona.Wilinska@pw.edu.pl

¹ Faculty of Civil Engineering, Mechanics and Petrochemistry, Institute of Chemistry, Warsaw University of Technology, Lukasiewiczza 17 St, 09-400 Plock, Poland

volume fly ash binders and geopolymers, has been developed. This binding material is composed of high amount of fly ash (at least 70 mass%) and Portland cement. Moreover, it is activated with alkaline media; thus, it can be considered as hybrid cement [7, 8, 10, 35–40]. It is important that in the case of hybrid cements, alkalinity may increase in situ as a result of chemical reaction, e.g., using Na_2SO_4 as an activator [5, 7, 38, 39].

Independently from the binding material considered, i.e., hybrid alkaline binder or geopolymer, it is essential to study what happens with aluminosilicate source material in the presence of alkaline activator: what is the way of development of its activity and what types of products are formed. It depends on the type of activator, conditions of hardening and features of the starting aluminosilicate material. Fly ashes can show significantly various properties and chemical compositions depending on technology of combustion, the type of coal, off-gas desulfurization technology, etc. [41–46]. Thus, there are differences in mechanism of their reactivity in alkaline media as well as in formed products.

In our previous works, we investigated, among others, the reactivity of fly ashes from different sources (conventional and fluidized combustion of coal) in the presence of water and in contact with $\text{Ca}(\text{OH})_2$ [43]. We described the influence of selected chemical admixtures on pozzolanic and hydraulic activities of different fly ashes from conventional combustion of coal [41] as well as the processes of early hydration of pastes containing typical or high amount of fly ash in the presence of selected activators [9, 47, 48]. Preliminary study concerning mechanical and combined (chemical + mechanical) activation of fly ash–cement mixtures, containing 80% of conventional fly ash and 20% of Portland cement, was also performed [10, 49]. Concretes containing 50% of conventional or fluidized fly ash as well as mixture of both of them as replacement of the cement were also investigated [50]. It was found that fluidized fly ash causes higher compressive strength of concrete compared to value registered for sample containing conventional one. Recently, we studied mixtures composed of fluidized fly ash and blast furnace slag as non-clinker binder in which fly ash was considered as activator for slag. Results of investigation of hydration products arising in such systems were presented in [51]. The results are promising and encourage further research of, e.g., activated systems containing a very high amount of fluidized fly ash and a small amount of cement. The knowledge about ways of development of fluidized fly ash activity in low and medium alkaline media as well as the kinds of formed products is important for such utilization of this material.

In this work, systems containing fly ash and solution of hydroxide (without cement) were studied. It was taken into

account that such species have more simple compositions than fly ash–cement binders. It makes the influence of alkalinity directly on fly ash possible to observe. However, the presence of cement can, to some degree, change chemical reactions by introducing additional reactive components. Cement can also undergo alkaline activation and some products of its hydration can react with fly ash (e.g., pozzolanic reaction). However, in the case of very high volume fly ash binders, cement is present in low amount only. Therefore, it is important to disclose changes in fly ash reactivity under the influence of alkaline media of different pH.

The aim of this study is to explore the influence of different alkali activators and temperature on the reactivity of two types of fly ash (conventional and fluidized). Fly ash formed in fluidized combustion installation shows significantly different properties compared to commonly used conventional fly ash. Fluidized fly ash has porous, irregular and no-vitreous grains. It contains Ca compounds in form of lime, anhydrite and calcium carbonate. Such properties of fluidized fly ash have been confirmed many times, e.g., in the papers [42, 52, 53]. This material undergoes reaction in the presence of water and has some self-cementing properties [43, 44, 52, 54, 55]. In the paste performed with it, at adequate high pH, ettringite may be formed. Hydrated calcium silicates (C–S–H¹ phase), gypsum and $\text{Ca}(\text{OH})_2$ may be also created [44, 54–56]. Therefore, this kind of fly ash seems to be interesting as the main component of binding mixture and can develop activity and form solid products at milder conditions of reaction than conventional fly ash. Thus, in this paper, alkali activated conventional fly ash was considered as a reference, while the main emphasis was put on activated fluidized fly ash as potential component of high or very high volume fly ash mixtures.

There are a lot of literature reports concerning the influence of alkaline media on conventional fly ash (e.g., [15, 16, 21, 26, 57–59]). There are also attempts of utilizing fluidized fly ash in a geopolymer [13, 53, 60–62] or alkali activated controlled low-strength material [63]. However, according to our knowledge, fluidized fly ash is not considered as the main component of alkali activated hybrid cement, so far. Moreover, there is rather lack of literature reports involving the impact comparison of the following factors on reactivity of fly ash and formed products: type of fly ash (conventional, fluidized), temperature of early reaction as well as kind of hydroxides used in range of low to moderate concentrations. Such comparison and detailed discussion are presented in this paper.

¹ Abbreviations used in cement chemistry: C–CaO, S–SiO₂, H–H₂O, A–Al₂O₃, N–Na₂O, K–K₂O.

Materials and methods

Materials

Fly ashes

Both fly ashes used in this research were produced in energy industry as by-products during hard coal combustion. The fly ash, denoted in further part of this paper as PK, came from conventional pulverized combustion. The second type of fly ash, marked further as PF, came from fluidized combustion installation.

Average oxide composition (main components) of PF and PK, the shape of their grains and pH value of water extracts (water to fly ash ratio equal 10: 1) are presented in Fig. 1. It can be seen that both fly ashes significantly differ in morphology of their grains. They are mostly spherical in the case of PK (it is a typical shape of grains for conventional pulverized fly ash) while PF is composed of grains which are irregular rather than spherically shaped. That is why PF exhibits higher water demand than PK. Both fly ashes have similar content of main constituents recalculated into oxides (i.e., $\text{SiO}_2 + \text{Al}_2\text{O}_3 + \text{Fe}_2\text{O}_3 > 75$ mass%); however, the amount of SiO_2 is slightly higher, while the amount of Al_2O_3 and Fe_2O_3 is lower for PF compared to PK. Moreover, for PF the content of CaO and SO_3 is, respectively, about two times and about five times higher, compared to composition of PK. Water extracts for the both materials are alkaline (pH above 11).²

X-ray diffraction patterns, IR spectra and TG/DTG results for PK and PF are presented in Figs. 2–4, respectively. There is a need to discuss these results here to make comparison of the results for raw and activated fly ashes as well as analyzing the process of their chemical transformations easier.

X-ray diffraction pattern (Fig. 2) shows the presence of quartz and mullite as the main crystalline components of PK; thus, it confirms results presented by us previously for conventional fly ash [41, 42]. In the case of PF, the presence of quartz is also visible; however, mullite is not present as a result of lower temperature of coal combustion. Moreover, PF contains anhydrite and calcite. Hematite is visible in PF, similarly as in PK. In the case of PF, the presence of crystalline aluminosilicate phase, probably type of muscovite, is registered. X-ray diffraction patterns confirm general differences in composition of fly ashes coming from conventional and fluidized combustion, and the results agree with literature data, e.g., [42, 51, 52, 54, 55].

IR spectra (Fig. 3) show very intense absorption bands located at range of wavenumbers from about 900 cm^{-1} to

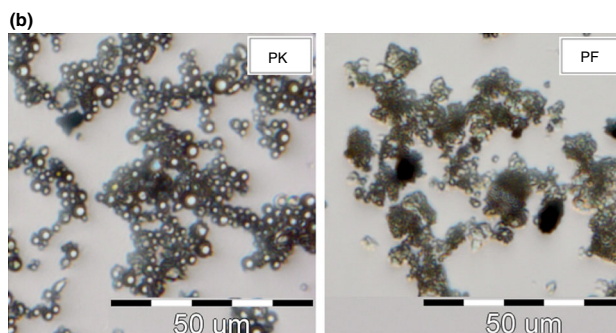
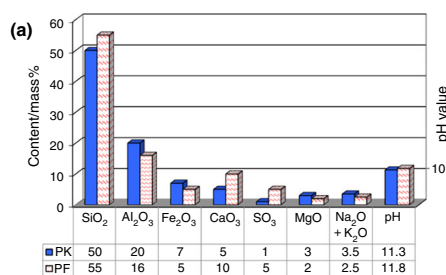


Fig. 1 Average oxide composition (main components) of fly ashes PK and PF, pH values of water extracts (a) and view of grains (b)

about 1300 cm^{-1} with extreme at 1067 cm^{-1} (for PK) and 1082 cm^{-1} (for PF). This effect is connected with vibrations of Si(Al)-O bonds (asymmetric stretching vibrations [58]) in silica and aluminosilicate phases. The band is related to overlapped effects characteristic for the following components of fly ashes: quartz (1150 cm^{-1} [57]), mullite (for PK only, $1180\text{--}1130\text{ cm}^{-1}$ [57, 58], the presence of mullite is also confirmed by band at about 555 cm^{-1} [21]) as well as amorphous silica which presence is confirmed by relatively large half-width of the band. Typical doublet for quartz is observed for both fly ashes at about 795 and 776 cm^{-1} [21]. A band at 457 cm^{-1} may be ascribed to bending vibrations of Si-O-Si in SiO_4 tetrahedra [58, 59]. In the case of PF, expected absorption band at about 1100 cm^{-1} related to SO_4^{2-} (three bands at $1200\text{--}1000\text{ cm}^{-1}$ in the case of anhydrite [64]) is not visible separately because it overlaps with the main broad fly ash band. However, several other bands of smaller intensity confirm the presence of calcium sulfate in form of anhydrite: 679 , 612 and 595 cm^{-1} [46, 64]. A few effects of small intensity show the presence of carbonates (CaCO_3) in PF: a band at about 1410 cm^{-1} and probably also a shoulder at about 880 cm^{-1} . The bands related to the presence of water (broad band with extreme at above 3440 cm^{-1} and weak band at 1604 cm^{-1}) are more intense for PF compared to PK. These results of reinvestigated fly ashes agree with the previously presented [41, 45].

TG/DTG curves registered for PK (Fig. 4a) disclose the presence of unburned carbon (the mass loss at temperature $500\text{--}730\text{ }^\circ\text{C}$ in the case of measurements carried out in air-oxidizing atmosphere). In the case of nitrogen (inert) gas

² PK fly ash of the same average oxide composition was previously used in our works [9, 45, 48, 50], PF fly ash in [45, 50].

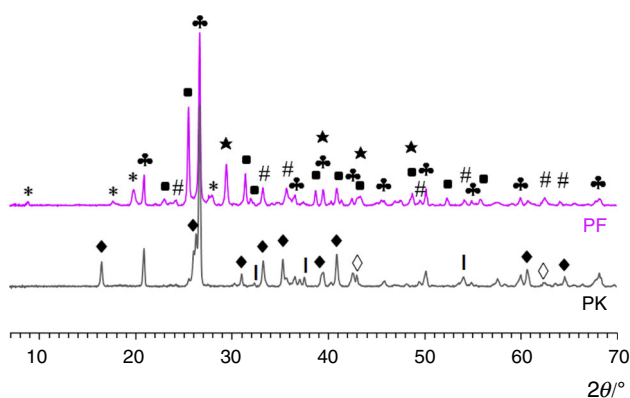


Fig. 2 X-ray diffraction patterns for PF and PK fly ashes (*—muscovite, ✕—quartz, ■—anhydrite, #—hematite, ★—calcite, ◇—MgO, I—CaO, ◆—mullite)

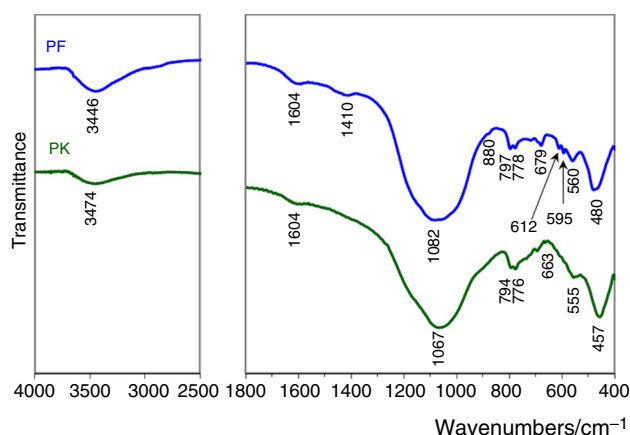


Fig. 3 IR spectra for PF and PK fly ashes

atmosphere, the mentioned mass loss is not observed while smaller continuous mass loss is registered at higher temperatures starting from 750 °C [41]. It is probably the effect of reduction of small amount of CaSO_4 and Fe_2O_3 with carbon and release of CO_2 in these reactions [65]. Very small effect up to 100 °C confirms that PK almost does not contain free water.

TG/DTG curves for raw PF (Fig. 4b) registered in nitrogen atmosphere show three main mass losses: first to 300 °C is about 1.5%, second from 300 to 550 °C is only about 0.5%, while from 550 to 1000 °C (the highest mass loss) is almost 9% (percentages with respect to initial mass of sample). Small mass loss at lower temperatures results mainly from evaporation of the adsorbed water from porous structure of fly ash grains. In the case of measurement in inert atmosphere, two effects of mass losses can be separated at high temperatures: mass loss at 550–650 °C—decomposition of carbonates (CaCO_3), and mass loss above 700 °C—reduction of CaSO_4 with carbon [65, 66]. Reduction of iron oxide is another reaction that may occur at high temperature [65]. The interpretation

presented above was confirmed by the course of TG and DTG curves registered in air. In the case of presence of oxygen, carbon is burned (similarly as for PK). This process is visible as significant mass loss at temperature above 500 °C. This effect partially overlaps with mass loss related to decomposition of carbonates. Above 730 °C there is lack of changes of mass in contrast to results registered in nitrogen. In such conditions reduction of CaSO_4 is not possible.

Chemical reagents

Two chemical reagents of analytical purity were used as alkaline activators: NaOH and KOH. Solutions of different concentrations of these hydroxides were performed: 0.1 M (low concentration) and 4.0 M (moderate concentration). We described the second concentration (i.e., 4.0 M) as moderate alkali one taking into account that much higher concentrations of hydroxides are usually used to create geopolymers, e.g., 8 M [30, 32, 58], 10 M [30, 32, 62] or 15 M [13, 61, 62].

Preparation of fly ash pastes

Fly ash pastes were performed by hand mixing adequate mass of fly ash and water solutions of hydroxides (0.1 M NaOH, 0.1 M KOH, 4 M NaOH, 4 M KOH). Two types of fly ash were used: PK and PF. The mass ratio of liquid to solid was 1: 1. Fly ash pastes were tightly closed in small polyethylene forms (cylindrical shape and volume of about 30 cm³) and kept under different temperature conditions:

- part of the samples was stored at room temperature,
- second part was kept at 60 °C during 24 h and at room temperature during the next days.

After eight days, hydration processes of all the samples were stopped by the use of acetone [9].

Methods of investigations

Thermal analysis was conducted using SDT 2960 Thermoanalyser (TA Instruments) at temperature range 20–1000 °C (heating rate 10 °C min⁻¹) and at nitrogen atmosphere (analyses of some samples were additionally performed at static air). Open alumina crucible was used; Al_2O_3 (corundum) was used as a reference. The sample mass was 9–13 mg. TG and DTG curves were registered.

IR spectra were collected by FTIR spectrophotometer Genesis II (Mattson) at 4000–400 cm⁻¹ wavenumbers. Samples were prepared as KBr pellets.

X-ray diffraction patterns were recorded using Cu-K α radiation on a Bruker D8 Advance diffractometer.

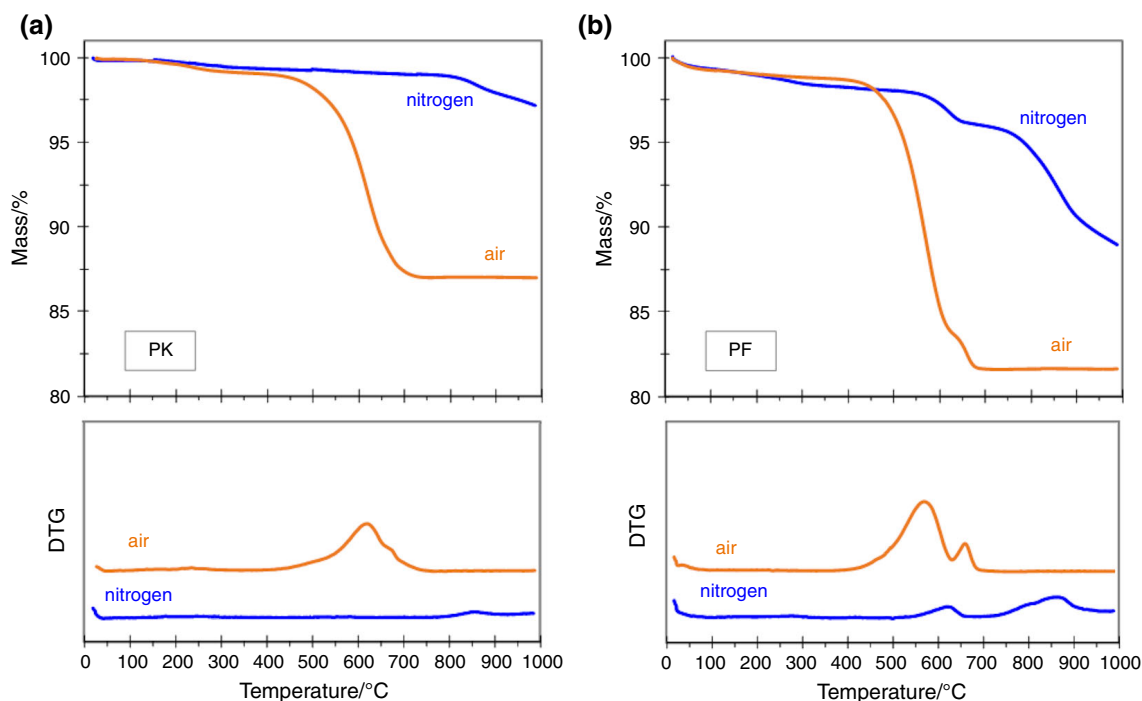


Fig. 4 TG and DTG curves for PK (a) and PF (b) registered at different gas atmosphere: air or nitrogen

Observations of grains of fly ashes were carried out by the use of optical microscope OLYMPUS BX41 in transmitted light.

Results and discussion

Influence of solutions of hydroxides and temperature on hydration of PK

Results of investigations of PK pastes were presented in figures: thermal analysis results—Fig. 5, IR spectra—Fig. 6, X-ray diffraction patterns—Fig. 7.

Low concentrated solutions of hydroxides

As one might expect, the pastes made with conventional fly ash do not undergo reaction in 0.1 M hydroxides, similarly as in the case of contact with water [43]. Solutions of 0.1 M NaOH and KOH provide pH = 13; thus, it was higher than pH of water-PK extracts (Fig. 1). However, TG/DTG results (Fig. 5) show only very small mass loss resulting from evaporation of water (less than 2% till 500 °C). The increase in the temperature of early hydration also has no significant effect on the reactivity of PK. The shapes of TG and DTG curves registered for raw PK (Fig. 4a) and for its paste (Fig. 5) at nitrogen atmosphere are quite similar. Only in the case of solution of NaOH and

reaction at room temperature the amount of bound water is slightly higher.

Similar conclusions can be drawn from IR spectra (Fig. 6). The registered results are almost the same as for raw PK (Fig. 3) irrespective of temperature of early reaction and type of liquid medium. Weak bands indicating the presence of carbonates ($1415\text{--}1450\text{ cm}^{-1}$) and water ($3420\text{--}3450\text{ cm}^{-1}$, $1615\text{--}1650\text{ cm}^{-1}$) appear. Only for the sample activated with 0.1 M NaOH, the presence of water bound in hydrates as well as some displacement of the main absorption band toward lower wavenumbers are visible (changes of position of the extreme of the band from about 1070 cm^{-1} (Fig. 3) to about 1035 cm^{-1}). It confirms TG/DTG results and indicates that in the presence of NaOH, dissolution of aluminosilicate species from fly ash and then formation of gel products happen a little easier than in the presence of KOH.

Summarizing, PK, due to its chemical and mineralogical composition, can react only to a very small degree and it does not show self-cementing properties. Solutions of the hydroxides used exhibit too low alkalinity to dissolve the grains of PK fast and in high amount which is necessary for transformation into hardened products.

Hydroxide solutions of moderate concentration

In the case of moderate concentration of solutions of hydroxides (4 M), used in this research, one should expect that the final material includes unreacted ash and reaction

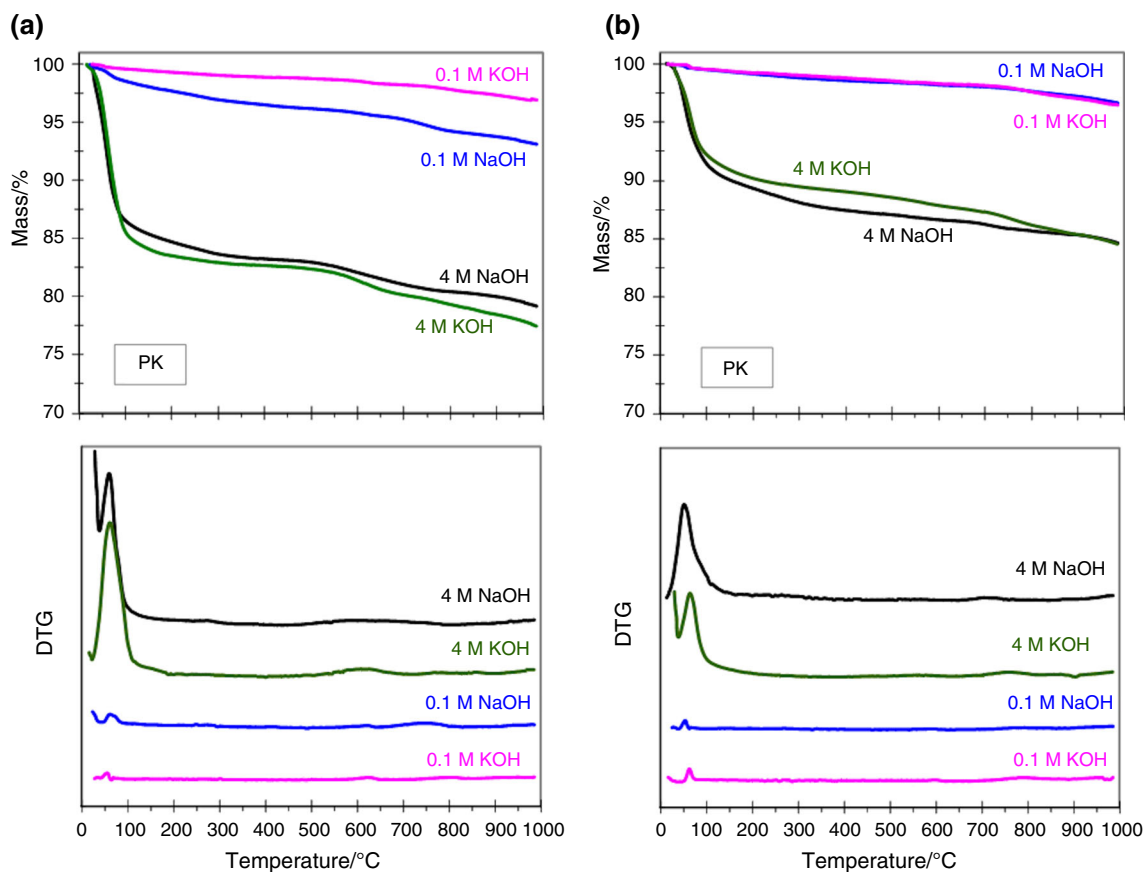


Fig. 5 TG and DTG curves for PK hydrated in solutions of hydroxides, **a** samples hydrated at room temperature, **b** samples hydrated at 60 °C for 24 h and at room temperature for next days (measurements at nitrogen atmosphere)

products (sodium or potassium aluminosilicate gel and/or crystalline aluminosilicates). Increasing concentration of hydroxide solution provides better conditions for dissolution of silicate and aluminate species from aluminosilicate source material. Generally, the ability to dissolve of aluminosilicate material increases along with the concentration of alkali solution [11]. In the case of high concentration of OH^- , polycondensation was hindered and aluminosilicate gel precipitates in the early stages [19].

Considering the above, it is not a surprise that the reaction degree of PK is higher when solutions of 4 M concentration are used compared to 0.1 M hydroxides. This is confirmed by the results of thermal studies (Fig. 5) as well as IR spectra (Fig. 6). In the case of 4 M solutions, significantly higher amount of water is bound in comparison with the situation when low concentrations of hydroxides were used (Fig. 5). PK fly ash hydrated at room temperature exhibits the presence of reaction products which can evaporate mainly to about 100 °C (evaporation of loosely bound water from aluminosilicate gel). In the case of sample kept at elevated temperature (60 °C/24 h) smaller mass loss connected with the presence of bound water is observed compared with results of paste hydrating

in lower temperature. Moreover, the mass loss occurs at broader temperature range (mainly to about 300 °C). It may indicate that higher temperature of reactions favors the polycondensation processes. Moreover, similar courses of TG/DTG curves recorded for 4 M NaOH and 4 M KOH show that not the kind of cation but rather the temperature of early hydration is crucial to amount of bound water and formed products in the analyzed case.

Occurrence of chemical reactions under the influence of 4 M hydroxides solutions is also confirmed in IR spectra. It is clearly visible comparing the IR results presented in Fig. 3 and in Fig. 6. In the case of PK paste, the main absorption band becomes sharper and its extreme is shifted to lower wavenumbers. Such changes of position of the band confirm the modification of chemical bonds in the aluminosilicate material. Amorphous phases of fly ash undergo reactions with hydroxides, and alkaline aluminosilicate gel is formed [59]. For samples hydrating with NaOH, the band with extreme at about 1005 cm^{-1} confirms the formation of sodium aluminosilicate gel (N–A–S–H) [57, 67]. In the case of sample hydrated in the presence of KOH, the band is placed at about 1010 cm^{-1} for sample reacting at elevated temperature and at about 1040 cm^{-1}

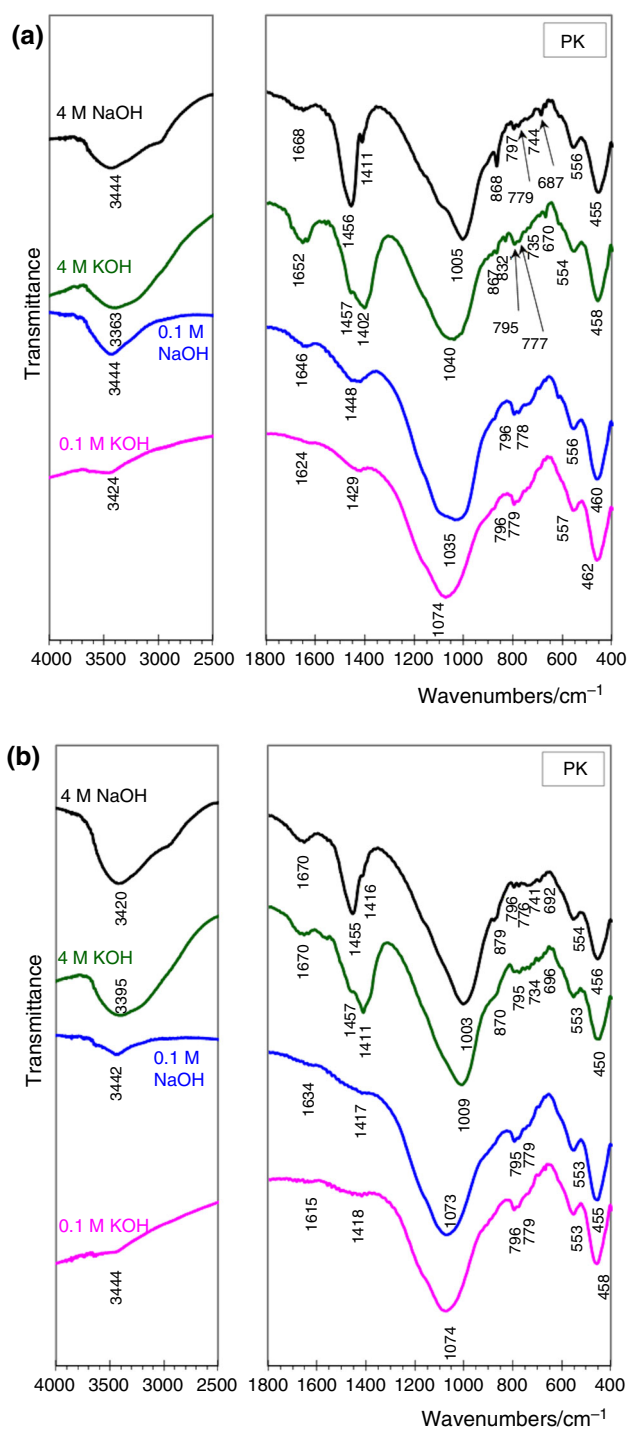


Fig. 6 IR spectra for PK hydrated in solutions of hydroxides, **a** samples hydrated at room temperature, **b** samples hydrated at 60 °C for 24 h and at room temperature for next days

for sample kept at room temperature. Such variability of position of the main absorption band shows the influence of cations on the networks and formation of aluminosilicate gel of different Si/Al ratio. Location of the band at higher wavenumbers indicates that reaction products contain

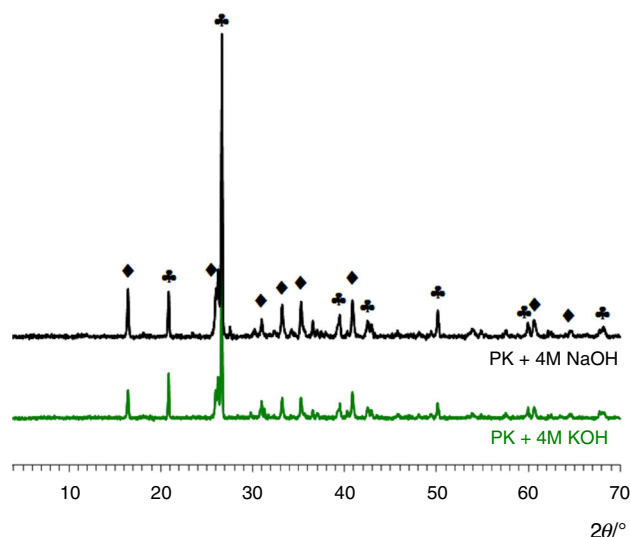


Fig. 7 X-ray diffraction patterns for PK hydrated in solutions of 4 M hydroxides (60 °C/24 h, room temperature for the next days); \blacklozenge —quartz, \blacklozenge —mullite

higher amount of Si compared to gel for which the band is located at lower wavenumbers (higher Si/Al ratio) [58, 59]. Broad band of stretching vibrations of water molecules and middle band of bending vibrations are also visible. There are small differences in the shape of this band registered for samples reacting in the presence of different hydroxides (e.g., a presence of shoulder at about 3000 cm^{-1} that is visible in the case of PK reacting in 4 M NaOH, but is not observed in the case of 4 M KOH). Clear absorption bands of carbonates at 1400–1500 cm^{-1} can also be observed. Their different positions and shapes indicate dependence of the formed carbonates on type of hydroxide solution. Comparison of the results with those obtained for samples hydrating in 0.1 M solutions shows that higher hydroxides concentration promotes carbonation processes. This process can take place rapidly at early stages of hydration [21]. As the investigated systems are poor in calcium, carbonate or bicarbonate salts of alkali may appear (in contrast to Portland cement paste in which CaCO_3 is created). A little alteration in nanostructure of N–A–S–H gel may also take place [68]. In the case of PK paste with 4 M NaOH two bands were registered: at about 1455 and smaller at about 1415 cm^{-1} which together with sharp band at 870–880 cm^{-1} may indicate the presence of sodium bicarbonate [21]. For comparison, in the presence of 4 M KOH the band at about 1400–1410 cm^{-1} and shoulder at about 1460 cm^{-1} are observed.

Small intensive doublet typical for quartz (800–770 cm^{-1}) is visible, which confirms the presence of unreacted fly ash in the samples. Used solutions and temperature hardly affect the bands at about 555 and about 455 cm^{-1} . A few new bands appear. In the case of 4 M

NaOH there are: weak band at about 740 cm^{-1} probably connected with octahedral Al [69], and band at about 690 cm^{-1} (stretching vibrations of Si–O–Al [32] related to new aluminosilicate product). In the case of 4 M KOH, for sample reacting at room temperature, band at 830 cm^{-1} (probably tetrahedral Al–O stretching [69]) and at 670 cm^{-1} can be seen.

Exemplary X-ray diffraction patterns (Fig. 7) collected for pastes hydrated in initially elevated temperature ($60\text{ }^{\circ}\text{C}/24\text{ h}$) show that results for PK paste are very similar to effects registered for raw fly ash (Fig. 2). The presence of quartz and mullite is visible confirming that these phases hardly reacted in 4 M solutions of hydroxides. There is no evidence of new crystalline products which could happen due to the presence of high pH solutions and elevated temperature. It confirms, in connection with other research results, that mainly amorphous aluminosilicate gel is formed.

Summarizing, PK fly ash, which does not react significantly in 0.1 M solutions, exhibits its reactivity in moderate (4 M) alkaline media. Amorphous aluminosilicate gel containing loosely bound water and carbonated phases are formed. Under the adopted research conditions, some amount of fly ash remains unreacted, crystalline quartz and mullite especially.

Influence of solutions of hydroxides and temperature on hydration of PF

Results of investigations of PF pastes are presented in figures: thermal analysis results—Figs. 8 and 9, IR spectra—Fig. 10, X-ray diffraction patterns—Fig. 11.

Low concentrated solutions of hydroxides

The results presented in this work proved that PF, in contrast to PK, exhibits reactivity in the presence of 0.1 M solution of hydroxide.

Thermal analysis results presented in Fig. 8 show that in the presence of 0.1 M solutions, PF forms hydration products which, especially for samples stored at room temperature, lose mass during heating mainly at temperature about $100\text{ }^{\circ}\text{C}$. The mass loss characterizing this process is relatively high in the case of 0.1 M NaOH (about 6.5% till $100\text{ }^{\circ}\text{C}$ and about 3.7% between 100 and $500\text{ }^{\circ}\text{C}$ for sample stored at room temperature). Position of the main DTG peak (near $100\text{ }^{\circ}\text{C}$) and the shape of TG (rapid mass loss at about $100\text{ }^{\circ}\text{C}$) indicate that ettringite [54, 70] is the main product of hydration. However, at similar temperatures, C–S–H phase undergoes dehydration; thus, these effects can overlap. Gypsum may also dehydrate at similar (slightly higher) temperature range, but the effects of its dehydration are not clearly visible (they may be

overlapping with other mass loss processes). Low intensity effect observed on DTG curves at about $110\text{ }^{\circ}\text{C}$ may indicate small amount of gypsum in the sample [54]. Dehydration of hydrated aluminosilicate and monosulphate phases is expected at higher temperatures. It is also visible in Fig. 8 that in adopted conditions of research, in the case of PF hydrated in KOH solution, mass loss corresponding to amount of water bound in hydrates is lower than in the case of NaOH. Moreover, in the case of PF hydrated in 0.1 M NaOH the effect of dehydration observed on DTG at about $100\text{ }^{\circ}\text{C}$ moved to slightly higher temperature compared to PF hydrated in 0.1 M KOH. It may not only be the effect of higher amount of water bound in ettringite-type phase but also the formation of greater amount of C–S–H in the presence of NaOH of low concentration, both for samples cured at room and at elevated temperature. This may be explained by higher solubility of aluminosilicate network in solution of NaOH, compared to KOH, and in this way better formation of hydrated products. Such information concerning higher extent of dissolution of different aluminosilicate materials when NaOH was used instead of KOH, may be found in several reports [11, 12, 14, 71].

Mass loss at about 400 – $500\text{ }^{\circ}\text{C}$, which would suggest the presence of $\text{Ca}(\text{OH})_2$ as a result of hydration of free CaO, is not separated on DTG as visible effect. It shows that available CaO reacted during 8 days of hydration and calcium sulfoaluminates (ettringite), calcium silicates and calcium aluminates could be formed.

Distinct mass loss at temperature above $500\text{ }^{\circ}\text{C}$ is a result of the presence of CaCO_3 and sulfates in the PF-paste sample (similar thermal effects as in the case of raw PF fly ash, Fig. 4b). In the case of hydrated PF, the mass loss at above $700\text{ }^{\circ}\text{C}$ comes from the presence of non-reacted anhydrite as well as release of this compound from thermal decomposition of ettringite [72]. This is why the effect of mass loss related to reduction of anhydrite with carbon is not significantly decreased despite binding some amount of anhydrite in sulfoaluminates.

Comparison of TG/DTG results for samples hydrated in different temperatures shows that when reactions take place at $60\text{ }^{\circ}\text{C}$ for 24 h, the formed products characterize by lower amount of bound water compared to those formed at room temperature. It is especially visible for sample PF + 0.1 M NaOH and indicates the influence of temperature on the formed products.

IR spectra (Fig. 10) and X-ray diffraction patterns (Fig. 11) also confirmed reactivity of PF in the presence of low concentrated hydroxides. Broad and intense band (Fig. 10) at wavenumbers from 3000 to 3700 cm^{-1} with extreme at about 3420 cm^{-1} and with some shoulders from the side of higher wavenumbers are visible (stretching vibrations of water molecules). Band of small intensity

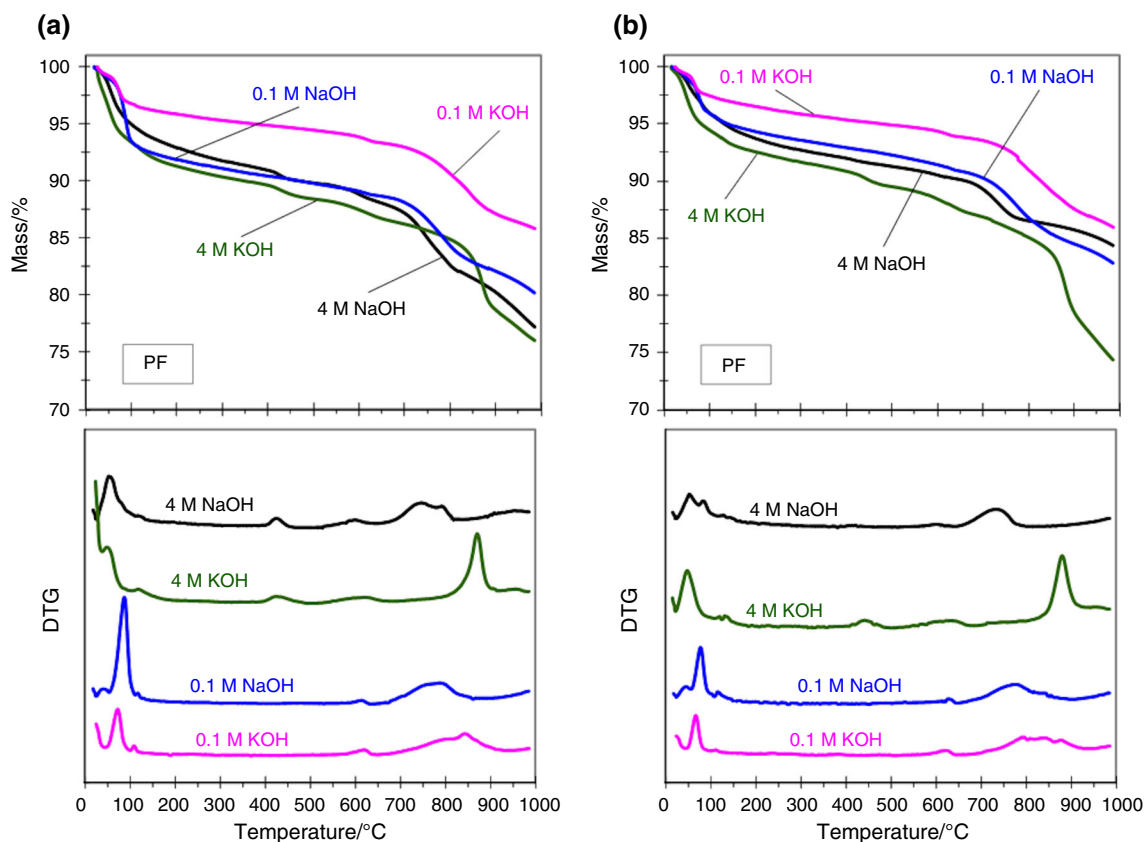


Fig. 8 TG and DTG curves for PF hydrated in solutions of hydroxides, **a** samples hydrated at room temperature, **b** samples hydrated at 60 °C for 24 h and at room temperature for next days (measurements at nitrogen atmosphere)

with an extreme at $1620\text{--}1635\text{ cm}^{-1}$ (deformational vibrations of H–O–H) is also observed. The main absorption band changes its shape compared to raw PF fly ash. In this broad band, an extreme at about 1105 cm^{-1} (anti-symmetrical stretching vibrations of SO_4^{2-} groups [73]) and shoulder from the side of lower wavenumbers are visible. It may indicate the presence of ettringite-like phases [73] and initiation of transformations in aluminosilicate phases. The shoulder (at about 1040 cm^{-1}) at the main band is slightly more pronounced for samples kept at elevated temperature for 24 h, which may indicate that raising temperature at early hydration periods favors reactions in aluminosilicate phases under alkaline conditions. The bands typical for anhydrite (at about 680 , 612 and 595 cm^{-1}) and quartz (at 778 and 797 cm^{-1}) are visible. It confirms that quartz remains unreacted and some amount of CaSO_4 is still available for reaction in further periods. This occurs due to the fact that CaSO_4 is probably in form of anhydrite II which is slightly soluble and reacts very slowly with water [74]. It can be seen, however, that for PF hydrated in 0.1 M NaOH these bands, characteristic for anhydrite, lost their intensities and, in the case of sample which was stored at room temperature, they almost

disappeared. Band at about 1445 cm^{-1} together with sharp effect at 875 cm^{-1} confirms the presence of carbonates.

X-ray diffraction patterns (Fig. 11) confirm that ettringite is formed in the systems in the presence of 0.1 M NaOH as well as KOH of the same concentration. The presence of non-reacted anhydrite is also registered which confirms conclusions from IR spectra. It is also visible that some amount of this component was transformed into gypsum. The effects indicating the presence of some other unreacted components coming from raw PF are also visible: quartz, hematite, calcite and small amount of crystalline aluminosilicate phase. There are no effects, both in X-ray diffraction patterns and in IR spectra, indicating the presence of $\text{Ca}(\text{OH})_2$. This compound did not precipitate. It confirms conclusions from thermal analysis.

Summarizing, one can state, that in the case of low concentrated solutions of alkali hydroxides, qualitative compositions of hydrated PF are similar despite different temperature of early hydration and various alkali cations in hydroxides. However, quantitative composition of samples may differ.

Higher reactivity of PF compared to PK in low concentrated solutions of hydroxides results from different chemical composition and dissolution ability of particular

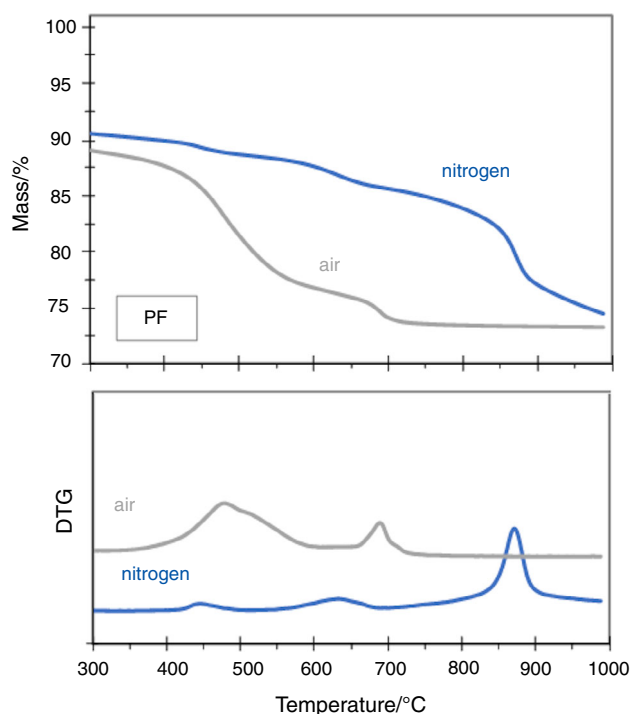


Fig. 9 Exemplary TG and DTG curves registered at temperature range above 300 °C for PF-4 M KOH paste at both oxidizing and inert atmosphere (sample after hydration at room temperature)

components. One can conclude that in the case of the investigated fly ashes, the key difference influencing products of hydration is availability of calcium and sulfate ions as well as structure of grains affecting the rate of aluminates and sulfate dissolution. Fly ashes used in this work are characterized by alkaline pH of water solution (pH above 11, Fig. 1), which may initiate dissolution of some components. Treating these fly ashes with solutions of hydroxides can rise pH of reaction medium and might provide alkaline conditions for further transformations. Especially, porous aluminosilicate materials of high reactivity, such as PF, contrary to the vitreous spherical grains of PK, may undergo dissolution in such conditions.

One would expect that raising temperature at early hydration periods can accelerate reactions in such a way that the same products but in higher amount can be formed. However, for example, while at room temperature ettringite is mainly formed, at elevated temperature the amount of ettringite may be lower and hydrated aluminosilicates are created, as it was evidenced in TG/DTG measurements. It may be caused, among others, by differences in solubility of particular compounds under different temperature and pH. Generally, it is known that solubility of most of chemical compounds in pure water rises as temperature grows up. Thus, at elevated temperature of early reaction and in the presence of NaOH, aluminate and silicate ions move into solution easier than at room temperature. One

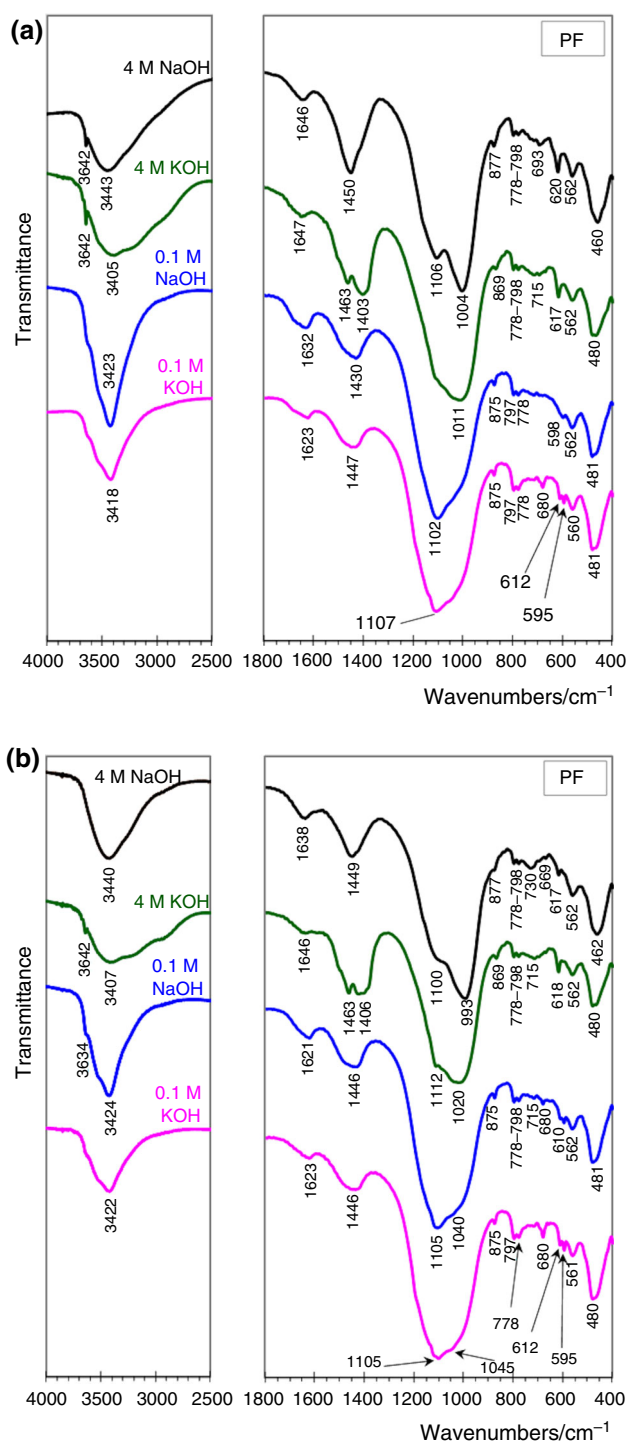


Fig. 10 IR spectra for PF hydrated in solutions of hydroxides, **a** samples hydrated at room temperature, **b** samples hydrated at 60 °C for 24 h and at room temperature for next days

can expect that aluminate ions appear in greater amount compared to silicate ions, because Al-O bonds exhibit lower bonding energy than Si-O and they are weaker and easier break than Si-O [57, 58]. However, it is well-known that solubility of CaO decreases at higher temperatures.

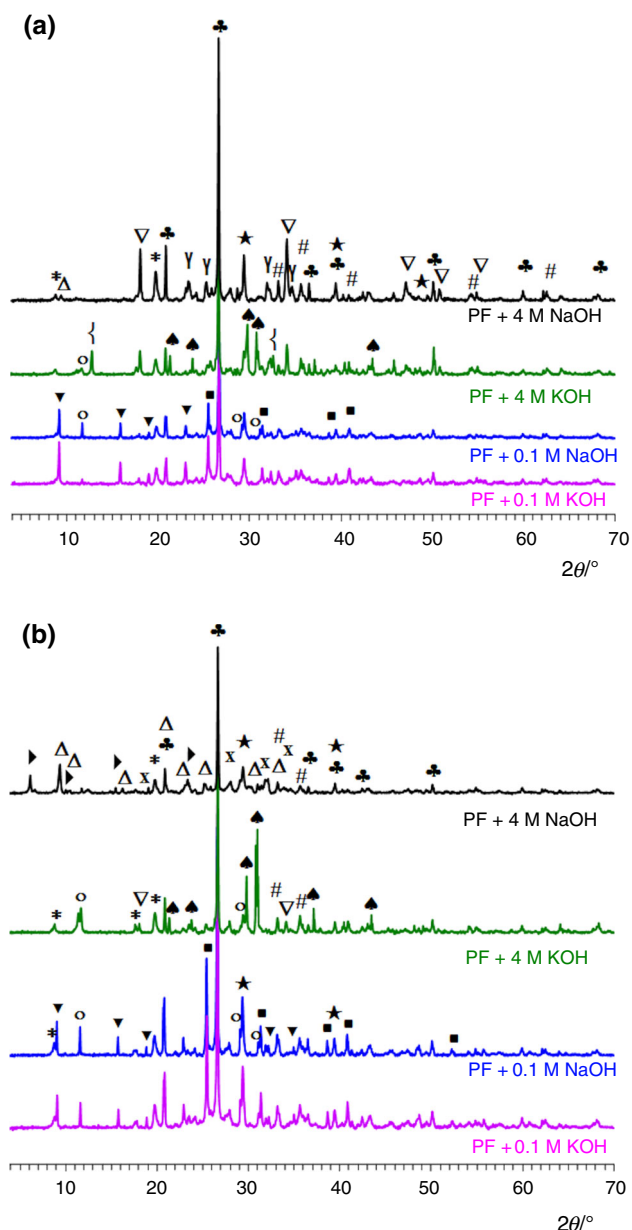


Fig. 11 X-ray diffraction patterns for PF after hydration in solutions of hydroxides, **a** samples hydrated at room temperature, **b** samples hydrated at 60 °C for 24 h and at room temperature for next days (*—muscovite, ♣—quartz, ■—anhydrite, #—hematite, ★—calcite, ♠—K₂SO₄, x—Na₂SO₄, ○—gypsum, ▽—Ca(OH)₂, Y—Na₄(SO₄)(CO₃, SO₄), burkeite, ▽—ettringite, {—potassium carbonate hydrate, Δ—zeolite, sodium aluminum silicate hydrate, ►—zeolite, calcium aluminum silicate hydrate)

Moreover, at increasing temperature, sulfate ions can be less available for ettringite formation because of their incorporation in C–S–H-type products [75]. This all could provide conditions which favor the creation of amorphous hydrates of aluminosilicates or other products containing lower amount of bound water than ettringite.

It was found that not only temperature but also the type of cation influences the formed products. Na⁺ and K⁺ ions may incorporate into the structure of hydrated products [21]. Moreover, in the case of PF, which in contrast to PK contains porous aluminosilicate grains, the activators may contribute to dissolution processes despite low concentration of solutions of hydroxide. It was mentioned above that solubility of aluminosilicate grains may be better in the case of NaOH compared to KOH. In the adopted conditions of the experiments, ettringite-type phase seems to be preferably formed in the presence of NaOH, possibly as an effect of better availability of aluminate ions. On the other hand, increasing solubility of aluminosilicate species in the presence of NaOH can lead to precipitation of higher amount of C–S–H- and C–A–S–H-type products. Because of overlapping dehydration effects for these phases as well as formation of amorphous products, it should be assumed that all of them may be responsible for a larger mass loss recorded at about 100 °C.

In general, increasing alkalinity favors retardation of ettringite formation. However, the effects of sodium or potassium and sulfate ions on the created products strictly depend on relative concentrations of these components [76]. For example Chindaprasirt et al. [62] observed ettringite in the case of hydration of fluidized fly ash in the presence of additional amount of Al(OH)₃ and high concentration (10 M) of NaOH, while it was not found in the case of 15 M NaOH. Brown and Bothe [77, 78] stated that in the case of hydration of tricalcium aluminate, tricalcium silicate and gypsum, ettringite is not formed in the presence of low concentration (0.5 M) of KOH and at elevated temperature.

Moderately concentrated solutions of hydroxides

Comparing the results obtained for PF reacting in 0.1 M and 4 M solutions, one may observe that in the presence of higher concentration some new formed phases appear while ettringite is not visible. Moreover, in the case of 4 M hydroxides, influence of type of cation as well as temperature of early hydration are more pronounced.

Thermal analysis results (Fig. 8) disclosed that mass loss registered up to 200 °C is similar for samples hydrated in 4 M NaOH, 4 M KOH as well as 0.1 M NaOH. However, reaction products created at solutions of higher alkalinity dehydrate at lower temperatures compared to products formed in low concentrated hydroxides. In the case of more alkaline media, aluminate and silicate species are easily dissolved and aluminosilicate gel is formed. Moreover, because of easier dissolution of aluminosilicate matrix, one can expect that in the presence of 4 M hydroxides the ratio of aluminate to sulfate ions in the solution is higher than in the case of processes occurring in

hydroxides of low concentration. Alkalinity is also higher. In such conditions ettringite-like phases are not formed. One of the reasons is the fact that stability of ettringite is dependent on pH [77, 79]. In the case of high alkaline solution, rather less crystalline phases of monosulfate and U-phase (sodium-substituted AF_m phase) [7, 79] or syngenite (in the case of KOH used) [78] are formed. It is also possible that sulfate ions were partially incorporated in the structure of aluminosilicate gel. Similar mechanism has also been suggested by other authors [80].

Comparison of the mass loss (up to 200 °C) for samples performed with PK (Fig. 5) and PF (Fig. 8) shows that in the presence of PF the amount of bound water is lower regardless of temperature of early reaction period. It may be, once again, related to the type of formed products containing different amount of water. Basing on information given in [81] one may state that the increase of amount of aluminate species causes faster condensation rate. It happens because reactions of condensation are initiated by Al [22]. Thus, basing only on oxide chemical composition (Fig. 1) of both investigated fly ashes, one may expect higher degree of condensation in the case of PK fly ash which contains a little higher amount of aluminate components than PF. However, in the case of PF these components are better available for reaction because of porous and non-vitreous structure of grains.

At about 420 °C, samples of PF hydrated in 4 M solutions of hydroxides exhibit small effect of mass loss on TG and DTG curves. This proves the presence of Ca(OH)₂ which precipitated under influence of high alkaline media. The effect is not observed in the case of PF after reaction in 4 M NaOH at early elevated temperature. Initially, in PF-hydroxides pastes, Ca²⁺ moves into the solution and then it precipitates in form of Ca(OH)₂, similarly as it was observed by Panagiotopoulou et al. in the case of slag [71]. The presence of Ca(OH)₂, which was not observed for pastes hydrated in 0.1 M solutions, suggests that in the case of higher concentrations of hydroxides, NaOH (KOH) reacts with CaSO₄ improving its solubility. Na₂SO₄ (or K₂SO₄, respectively) may be formed in this reaction and slightly soluble Ca(OH)₂ can precipitate [62, 82]. In the case of 4 M NaOH (60 °C/24 h) the absence of Ca(OH)₂ indicates higher degree of reaction and involvement of calcium in aluminosilicate products.

At temperatures above 550 °C an intense mass loss is observed. A few processes can occur at this temperature range, i.e., decomposition of CaCO₃ (at 600–700 °C) and reduction of sulfates and Fe₂O₃ (at higher temperatures), similarly as in the case of raw PF (Fig. 4b) and PF after reaction in 0.1 M solutions (Fig. 8). It is visible that concentration of hydroxide and its type influence mass loss and shape of DTG at this high-temperature range. Relatively small mass loss is observed at about 600 °C and a bigger

mass loss at higher temperatures. This effect above 750 °C is especially visible in the case of PF hydrated in KOH solution (clear DTG peak at temperature near 900 °C). This mass loss may be an effect of the presence of sulfates (including also K₂SO₄) in the sample and their reduction with carbon. Another processes occurring in this temperature range can be related to the presence of carbonated hydroxides (alkaline hydroxides are easily carbonated with CO₂ from air). Both of the types of components (sulfates, alkali carbonates) can give mass loss at high temperatures. In general, alkaline carbonates are stable at high temperatures and do not decompose or only slightly decompose at temperature up to 1000 °C. Kim and Lee [83] reported that pure Na₂CO₃ starts to undergo very slow decomposition at temperatures higher than its melting point (850 °C). However, in the presence of carbon black the rate of decomposition process of Na₂CO₃ is enhanced as a result of reaction between this carbonate and carbon at temperatures above 800 °C [83]. Pure K₂CO₃ is stable up to temperature about 900 °C (melting point), and it can volatilize near this temperature [84]. Exemplary TG/DTG results registered at temperature range above 300 °C for PF-4 M KOH paste at both oxidizing and inert atmosphere (Fig. 9) indicate that high temperature processes involving carbon are responsible for this observed significant mass loss.

X-ray diffraction patterns (Fig. 11) confirm appearance of some amounts of Na₂SO₄ and K₂SO₄ in the samples in the presence of NaOH and KOH, respectively, while IR spectra (Fig. 10) show changes in carbonate phases under influence of hydroxides of moderate concentration. These both techniques also confirm precipitation of some amount of Ca(OH)₂ as well as changes in aluminosilicate matrix. The presence of non-reacted quartz is also visible.

X-ray results (Fig. 11) show that reaction processes go differently in the presence of various hydroxides as well as at different conditions of early hydration. In the case of PF hydrated in 4 M NaOH at early elevated temperature, the presence of zeolites type of calcium aluminum silicate hydrate and sodium aluminum silicate hydrate are visible. Creation of such products is important, e.g., from the point of view of durability of material containing PF as well as possibility of its utilization, for example for immobilization of heavy metals [85, 86]. In the case of PF hydrated in 4 M NaOH but at room temperature crystalline aluminosilicate products are not formed (weak effect at 2θ about 9.6 may indicate initiation of formation of such reaction product but it is difficult to identify it). For both temperature conditions of reaction, the presence of anhydrite and gypsum is not visible. The presence of Na₂SO₄ is registered for sample kept at elevated temperature, but it is poorly differentiated. It indirectly confirms that sulfate ions are incorporated into amorphous aluminosilicate gel; however, double sodium

salts type of burkeite may also be formed. Information about incorporation of sulfate ions in products type of C–S–H (for example by adsorption) [75] or in polymeric network of geopolymer-type gel [80] can be found in the literature. The presence of precipitated $\text{Ca}(\text{OH})_2$ is not visible in the case of sample hydrated at elevated temperature, while it is clear in the case of paste held at room temperature. Such results confirm findings obtained from TG/DTG curves.

In the case of PF treated with 4 M KOH, crystalline aluminosilicates are not formed. The presence of syngenite is also not confirmed. It is visible that crystalline K_2SO_4 (in the presence of 4 M KOH) is formed in clearly bigger amount than Na_2SO_4 (in the presence of 4 M NaOH). Potassium carbonate hydrate may also be created. Thus, one can conclude that Na^+ ions are preferably incorporated in solid aluminosilicate products while K^+ ions more preferably form other salts, K_2SO_4 especially. In the case of 4 M KOH, the presence of crystalline gypsum is visible. It was also confirmed, for both used hydroxides, that crystalline ettringite is not formed in adopted conditions.

The presence of $\text{Ca}(\text{OH})_2$ is confirmed in X-ray diffraction patterns for PF + 4 M KOH both for hydration at room temperature as well as at 60 °C/24 h. Thus, this component can react in a later period of hydration process, similarly as in the case of PF + 4 M NaOH hydrated at room temperature. In the case of PF hydrated in 4 M NaOH at early elevated temperature, the reaction processes are more advanced and Ca^{2+} was incorporated into aluminosilicate forms, zeolitic type as well as probably also in amorphous phases type of C–A–S–H or C–S–H. Sodium-based zeolite can be formed in such conditions. Obtained results confirmed that zeolite formation is preferred in the case of sodium activation unlike potassium activation [28]. The effect of temperature also cannot be ignored (higher temperature favors crystallization).

IR spectra (Fig. 10) registered for PF pastes hydrating in the presence of solutions of 4 M KOH and 4 M NaOH also confirm that this type of fly ash reacts in different ways compared to conventional fly ash; moreover, the differences resulting from type of hydroxide are more pronounced than in the case of PK. The main absorption band moves to lower wavenumbers, similarly as in the case of PK, confirming transformations in aluminosilicate phases. In the case when PF reacts in 4 M NaOH, the main sharp extreme is located at about 993 cm^{-1} for sample hydrated at elevated temperature and at about 1005 cm^{-1} for sample stored at room temperature. This shifting of the main band position may indicate increased incorporation of Al^{3+} and Ca^{2+} into tetrahedrally coordinated framework [87]. The effect visible at about 1105 cm^{-1} may be related to sulfate phases (vibrations of SO_4^{2-} groups) or quartz (Si–O–Si vibrations). The latter one is additionally confirmed by the

presence of doublet at 800–770 cm^{-1} . The differences in shape of the band of stretching vibrations of water molecules confirming differences in hydration products are also visible. Additional peak at 3642 cm^{-1} indicates the presence of $\text{Ca}(\text{OH})_2$. The exception is sample with 4 M NaOH stored at elevated temperature (similarly as in the case of TG/DTG and X-ray results). Because of the presence of $\text{Ca}(\text{OH})_2$ in the samples, formation of C–S–H phase together with N(K)–A–S–H gel may be expected; however, this cannot be proven by FTIR spectra because of overlapping of absorption bands (typical band position of C–S–H gel is about $970 \pm 5 \text{ cm}^{-1}$ and it shifts toward lower wavenumbers with increase of Ca/Si ratio [67]). Similarly as in the case of PK treated with 4 M solutions, in the case of PF a new band at about 715–730 cm^{-1} appears. This band is more pronounced for PF samples compared to PK which may indicate that more aluminosilicate Al-rich and/or Ca-rich products were formed. The presence of intense band at 993 cm^{-1} as well as a new band at 730 cm^{-1} are characteristic for alkaline aluminosilicates [15]. One more band at about 617–620 cm^{-1} appears. Most likely it is connected with the presence of sulfate products, e.g., K_2SO_4 in the case of sample treated with KOH. However, location of this band (about 620 cm^{-1}) as well as the band at about 730 cm^{-1} may also be connected with the presence of zeolitic forms (vibrational bands of O–Si–O bonds zeolite species) [21]. It is especially probable in the case of PF hydrated in 4 M NaOH (60 °C/24 h) for which X-ray analysis indicates only traces of Na_2SO_4 and the presence of calcium and sodium zeolites.

Different types of alkaline activators also influence carbonate phases as it was mentioned above. It is evidenced by shape of carbonate bands. In the case of PF treated by 4 M NaOH, there are likely calcium carbonate together with sodium carbonate, which is indicated by extreme of the most characterized band at about 1450 cm^{-1} and band at about 875 cm^{-1} . The band at 1450 cm^{-1} is typical for alkaline carbonates [21], Na_2CO_3 in this case. In the case of sample with KOH two bands at about 1463 and 1405 cm^{-1} and a band at 869 cm^{-1} are observed indicating the presence of hydrated potassium carbonate.

Conclusions

1. During hydration/activation of fly ash in alkaline media different products can be formed depending on: the kind of fly ash, concentration of alkaline solution, type of cation as well as temperature of early reaction.
2. The key factors influencing products of hydration of fly ash in low-concentration (0.1 M) hydroxides are: availability of calcium and sulfate ions as well as

structure of grains affecting the rate of aluminate and sulfate dissolution. Conventional fly ash almost does not react at such conditions. Reactivity of fluidized fly ash in 0.1 M solutions of hydroxides was confirmed.

3. Fluidized fly ash reacts in similar way in 0.1 M solutions of hydroxides independently from type of cation (Na^+ or K^+) and temperature of early hydration (room temperature or 60 °C/24 h). It means that qualitative compositions of PF pastes are similar but quantitative compositions can be different.
4. In the case of fluidized fly ash hydrated in 0.1 M solutions of hydroxides, ettringite-type phases are mainly formed. Other products of hydration (amorphous hydrated aluminosilicates) probably form more easily in the case of 0.1 M NaOH compared to 0.1 M KOH.
5. Moderate concentration of hydroxides (4 M) is sufficient for initiation of reaction of both investigated fly ashes. In the case of conventional pulverized fly ash, amorphous aluminosilicate gel containing loosely bound water appears. In the case of fluidized fly ash, reaction process is more advanced and the formed products are characterized by higher degree of condensation of aluminosilicate species. Elevated temperature of early reaction favors polycondensation processes.
6. In the case of fluidized fly ash treated with 4 M hydroxides, contrary to the 0.1 M solutions, formed products strictly depend on the type of hydroxides and temperature of early hydration. Anhydrite and aluminates are better soluble in high alkaline media as compared to solutions of low concentrations; however, ettringite is not formed in such conditions. Sulfate ions are incorporated into other hydration products. $\text{Ca}(\text{OH})_2$, which may undergo further reaction in later hydration periods, precipitates.
7. The best conditions of reaction of fluidized fly ash are: elevated temperature of early reaction and 4 M NaOH. In such conditions not only amorphous aluminosilicate gel but also zeolites type of sodium aluminum silicate hydrate and calcium aluminum silicate hydrate are formed. Small amount of Na_2SO_4 and carbonated forms are created. In the case of 4 M KOH, both at room and at elevated temperature, zeolitic products are not present, while K^+ ions formed K_2SO_4 and potassium carbonate hydrate.
8. This work may be considered as preliminary research (the first step) for alkali activated hybrid cement containing very high amount of fluidized fly ash and low amount of cement. It seems to be beneficial to continue the research to explain influence of alkali activators on mixture fluidized fly ash–cement.

Open Access This article is distributed under the terms of the Creative Commons Attribution 4.0 International License (<http://creativecommons.org/licenses/by/4.0/>), which permits unrestricted use, distribution, and reproduction in any medium, provided you give appropriate credit to the original author(s) and the source, provide a link to the Creative Commons license, and indicate if changes were made.

References

1. Bouzoubaâ N, Zhang MH, Bilodeau A, Malhotra VM. Laboratory-produced high-volume fly ash blended cements: physical properties and compressive strength of mortars. *Cem Concr Res*. 1998;28:1555–69.
2. Arezoumandi M, Volz JS, Ortega CA, Myers JJ. Effect of total cementitious content on shear strength of high-volume fly ash concrete beams. *Mater Des*. 2013;46:301–9.
3. Lam L, Wong YL, Poon CS. Degree of hydration and gel/space ratio of high-volume fly ash/cement systems. *Cem Concr Res*. 2000;30:747–56.
4. Nguyen H-A, Chang T-P, Shih J-Y, Chen C-T, Nguyen T-D. Influence of circulating fluidized bed combustion (CFBC) fly ash on properties of modified high volume low calcium fly ash (HVFA) cement paste. *Constr Build Mater*. 2015;91:208–15.
5. Hemalatha T, Ramaswamy A. A review on fly ash characteristics—towards promoting high volume utilization in developing sustainable concrete. *J Clean Prod*. 2017;147:546–59.
6. Huang C-H, Lin S-K, Chang C-S, Chen H-J. Mix proportions and mechanical properties of concrete containing very high-volume of Class F fly ash. *Constr Build Mater*. 2013;46:71–8.
7. Donatello S, Fernández-Jiménez A, Palomo A. Very high volume fly ash cements. Early age hydration study. Using Na_2SO_4 as an activator. *J Am Ceram Soc*. 2013;96:900–6.
8. Donatello S, Palomo A, Fernández-Jiménez A. Durability of very high volume fly ash cement pastes and mortars in aggressive solutions. *Cem Concr Compos*. 2013;38:12–20.
9. Wilińska I, Pacewska B. Calorimetric and thermal analysis studies on the influence of waste aluminosilicate catalyst on the hydration of fly ash–cement paste. *J Therm Anal Calorim*. 2014;116:689–97.
10. Wilińska I, Pacewska B. Influence of selected activating methods on hydration processes of mixtures containing high and very high amount of fly ash. A review. *J Therm Anal Calorim*. 2018;33:823–43.
11. Xu H, van Deventer JSJ. The geopolymerisation of aluminosilicate minerals. *Int J Miner Process*. 2000;59:247–66.
12. Komnitsas K, Zaharaki D. Geopolymerisation: a review and prospects for the minerals industry. *Miner Eng*. 2007;20:1261–77.
13. Xu H, Li Q, Shen L, Wang W, Zhai J. Synthesis of thermostable geopolymer from circulating fluidized bed combustion (CFBC) bottom ashes. *J Hazard Mater*. 2010;175:198–204.
14. Duxson P, Fernández-Jiménez A, Provis JL, Lukey GC, Palomo A, van Deventer JSJ. Geopolymer technology: the current state of the art. *J Mater Sci*. 2007;42:2917–33.
15. Khale D, Chaudhary R. Mechanism of geopolymerization and factors influencing its development: a review. *J Mater Sci*. 2007;42:729–46.
16. Ma Y, Hu J, Ye G. The effect of activating solution on the mechanical strength, reaction rate, mineralogy, and microstructure of alkali-activated fly ash. *J Mater Sci*. 2012;47:4568–78.
17. Tchadjie LN, Ekolu SO. Enhancing the reactivity of aluminosilicate materials toward geopolymer synthesis. *J Mater Sci*. 2018;53:4709–33.

18. Andini S, Cioffi R, Colangelo F, Grieco T, Montagnaro F, Santoro L. Coal fly ash as raw material for the manufacture of geopolymer-based products. *Waste Manag.* 2008;28:416–23.
19. Somna K, Jaturapitakkul C, Kajitvichyanukul P, Chindaprasirt P. NaOH-activated ground fly ash geopolymer cured at ambient temperature. *Fuel.* 2011;90:2118–24.
20. Prud'homme E, Michaud P, Joussein E, Clacens J-M, Rossignol S. Role of alkaline cations and water content on geomaterial foams: monitoring during formation. *J Non Cryst Solids.* 2011;357:1270–8.
21. Criado M, Palomo A, Fernández-Jiménez A. Alkali activation of fly ashes. Part 1: effect of curing conditions on the carbonation of the reaction products. *Fuel.* 2005;84:2048–54.
22. Peng Z, Vance K, Dakhane A, Marzke R, Neithalath N. Microstructural and ^{29}Si MAS NMR spectroscopic evaluations of alkali cationic effects on fly ash activation. *Cem Concr Compos.* 2015;57:34–43.
23. Nath P, Sarker PK. Use of OPC to improve setting and early strength properties of low calcium fly ash geopolymer concrete cured at room temperature. *Cem Concr Compos.* 2015;55:205–14.
24. Sturm P, Gluth GJG, Simon S, Brouwers HJH, Kühne H-C. The effect of heat treatment on the mechanical and structural properties of one-part geopolymer-zeolite composites. *Thermochim Acta.* 2016;635:41–58.
25. Nazari A, Sanjayan JG. Synthesis of geopolymer from industrial wastes. *J Clean Prod.* 2015;99:297–304.
26. Hajimohammadi A, van Deventer JSJ. Dissolution behavior of source materials for synthesis of geopolymer binders: a kinetic approach. *Int J Miner Process.* 2016;153:80–6.
27. Meftah M, Oueslati W, Chorfi N, Amara ABH. Intrinsic parameters involved in the synthesis of metakaolin based geopolymer: microstructure analysis. *J Alloy Compd.* 2016;688:946–56.
28. Desbats-Le Chequer C, Frizon F. Impact of sulfate and nitrate incorporation on potassium and sodium-based geopolymers: geopolymerization and materials properties. *J Mater Sci.* 2011;46:5657–64.
29. Wan Q, Rao F, Song S, García RE, Estrella RM, Patiño CL, Zhang Y. Geopolymerization reaction, microstructure and simulation of metakaolin-based geopolymers at extended Si/Al ratios. *Cem Concr Compos.* 2017;79:45–52.
30. Zhang Z, Wang H, Provis JL, Bullen F, Reid A, Zhu Y. Quantitative kinetic and structural analysis of geopolymers. Part 1. The activation of metakaolin with sodium hydroxide. *Thermochim Acta.* 2012;539:23–33.
31. Pavithra P, Srinivasula Reddy M, Dinakar P, Hanumantha Rao B, Satpathy BK, Mohanty AN. A mix design procedure for geopolymer concrete with fly ash. *J Clean Prod.* 2016;133:117–25.
32. Djobo JNY, Elimbi A, Tchakoute HK, Kumar S. Reactivity of volcanic ash in alkaline medium, microstructural and strength characteristics of resulting geopolymers under different synthesis conditions. *J Mater Sci.* 2016;51:10301–17.
33. Castaldelli VN, Moraes JCB, Akasaki JL, Melges JLP, Monzó J, Borrachero MV, Soriano L, Payá J, Tashima MM. Study of the binary system fly ash/sugarcane bagasse ash (FA/SCBA) in $\text{SiO}_2/\text{K}_2\text{O}$ alkali-activated binders. *Fuel.* 2016;174:307–16.
34. Duan P, Yan C, Zhou W. Influence of partial replacement of fly ash by metakaolin on mechanical properties and microstructure of fly ash geopolymer paste exposed to sulfate attack. *Ceram Int.* 2016;42:3504–17.
35. García-Lodeiro I, Fernandez-Jiménez A, Palomo A. Hydration kinetics in hybrid binders: early reaction stages. *Cem Concr Compos.* 2013;39:82–92.
36. García-Lodeiro I, Fernández-Jiménez A, Palomo A. Variation in hybrid cements over time. Alkaline activation of fly ash–portland cement blends. *Cem Concr Res.* 2013;52:112–22.
37. Alahrahe S, Winnefeld F, Champenois J-B, Hesselbarth F, Lothenbach B. Chemical activation of hybrid binders based on siliceous fly ash and Portland cement. *Cem Concr Compos.* 2016;66:10–23.
38. Donatello S, Maltseva O, Fernández-Jimenez A, Palomo A. The early age hydration reactions of a hybrid cement containing a very high content of coal bottom ash. *J Am Ceram Soc.* 2014;97:929–37.
39. Garcia-Lodeiro I, Donatello S, Fernandez-Jimenez A, Palomo A. Hydration of hybrid alkaline cement containing a very large proportion of fly ash: a descriptive model. *Materials.* 2016;9:605.
40. Kulasuriya C, Vimonsatit V, Dias WPS, De Silva P. Design and development of alkali pozzolan cement (APC). *Constr Build Mater.* 2014;68:426–33.
41. Pacewska B, Wilińska I. Comparative investigations of influence of chemical admixtures on pozzolanic and hydraulic activities of fly ash with the use of thermal analysis and infrared spectroscopy. *J Therm Anal Calorim.* 2015;120:119–27.
42. Pacewska B, Blonkowski G, Wilińska I. Investigations of the influence of different fly ashes on cement hydration. *J Therm Anal Calorim.* 2006;86:179–86.
43. Pacewska B, Blonkowski G, Wilińska I. Studies on the pozzolanic and hydraulic properties of fly ashes in model systems. *J Therm Anal Calorim.* 2008;94:469–76.
44. Iribarne J, Iribarne A, Blondin J, Anthony EJ. Hydration of combustion ashes—a chemical and physical study. *Fuel.* 2001;80:773–84.
45. Pacewska B, Wilińska I, Nowacka M. Studies on the influence of different fly ashes and Portland cement on early hydration of calcium aluminate cement. *J Therm Anal Calorim.* 2011;106:859–68.
46. Mozgawa W, Król M, Dyczek J, Deja J. Investigation of the coal fly ashes using IR spectroscopy. *Spectrochim Acta Part A Mol Biomol Spectrosc.* 2014;132:889–94.
47. Pacewska B, Wilińska I, Blonkowski G. Investigations of cement early hydration in the presence of chemically activated fly ash. Use of calorimetry and infrared absorption methods. *J Therm Anal Calorim.* 2008;93:769–76.
48. Pacewska B, Wilińska I. Hydration of cement composites containing large amount of waste materials. *Procedia Eng.* 2013;57:53–62.
49. Wilińska I, Pacewska B. Zastosowanie kalorymetrii we wstępnych badaniach aktywowanych mieszanek popiołowo-cementowych. *Przem Chem.* 2017;96:761–5 (in Polish).
50. Kubissa W, Wilińska I, Pałuba M. Badanie właściwości betonów cementowych wykonanych z udziałem odpadów przemysłowych. *Prz Bud.* 2013;1:35–9 (in Polish).
51. Kledyński Z, Machowska A, Pacewska B, Wilińska I. Investigation of hydration products of fly ash–slag pastes. *J Therm Anal Calorim.* 2017;130:351–63.
52. Li X-G, Chen Q-B, Huang K-Z, Ma B-G, Wu B. Cementitious properties and hydration mechanism of circulating fluidized bed combustion (CFBC) desulfurization ashes. *Constr Build Mater.* 2012;36:182–7.
53. Chindaprasirt P, Rattanasak U. Utilization of blended fluidized bed combustion (FBC) ash and pulverized coal combustion (PCC) fly ash in geopolymer. *Waste Manag.* 2010;30:667–72.
54. Lee Seung-Heun, Kim Guen-Su. Self-cementitious hydration of circulating fluidized bed combustion fly ash. *J Korean Ceram Soc.* 2017;54:128–36.
55. Sheng G, Li Q, Zhai J. Investigation on the hydration of CFBC fly ash. *Fuel.* 2012;98:61–6.
56. Shen Y, Qian J, Zhang Z. Investigations of anhydrite in CFBC fly ash as cement retarders. *Constr Build Mater.* 2013;40:672–8.

57. Criado M, Fernández-Jiménez A, Palomo A. Alkali activation of fly ash: effect of the $\text{SiO}_2/\text{Na}_2\text{O}$ ratio, part I: FTIR study. *Microporous Mesoporous Mater.* 2007;106:180–91.
58. Fernández-Jiménez A, Palomo A. Mid-infrared spectroscopic studies of alkali-activated fly ash structure. *Microporous Mesoporous Mater.* 2005;86:207–14.
59. Fernández-Jiménez A, Palomo A. Composition and microstructure of alkali activated fly ash binder: effect of the activator. *Cem Concr Res.* 2005;35:1984–92.
60. Li Q, Xu H, Li F, Li P, Shen L, Zhai J. Synthesis of geopolymer composites from blends of CFBC fly and bottom ash. *Fuel.* 2012;97:366–72.
61. Chindaprasirt P, Paisitsrisawat P, Rattanasak U. Strength and resistance to sulfate and sulfuric acid of ground fluidized bed combustion fly ash–silica fume alkali-activated composite. *Adv Powder Technol.* 2014;25:1087–93.
62. Chindaprasirt P, Thaiwitaroen S, Kaewpirom S, Rattanasak U. Controlling ettringite formation in FBC fly ash geopolymer concrete. *Cem Concr Compos.* 2013;41:24–8.
63. Park SM, Lee NK, Lee HK. Circulating fluidized bed combustion ash as controlled low-strength material (CLSM) by alkaline activation. *Constr Build Mater.* 2017;156:728–38.
64. Mandal PK, Mandal TK. Anion water in gypsum ($\text{CaSO}_4 \cdot 2\text{H}_2\text{O}$) and hemihydrate ($\text{CaSO}_4 \cdot 1/2\text{H}_2\text{O}$). *Cem Concr Res.* 2002;32:313–6.
65. Payá J, Monzó J, Borrachero MV, Perris E, Amahjour F. Thermogravimetric methods for determining carbon content in fly ashes. *Cem Concr Res.* 1998;28:675–86.
66. van der Merwe EM, Strydom CA, Potgieter JH. Thermogravimetric analysis of the reaction between carbon and $\text{CaSO}_4 \cdot 2\text{H}_2\text{O}$, gypsum and phosphogypsum in an inert atmosphere. *Thermochim Acta.* 1999;340–341:431–7.
67. García-Lodeiro I, Fernández-Jiménez A, Blanco MT, Palomo A. FTIR study of the sol–gel synthesis of cementitious gels: C–S–H and N–A–S–H. *J Sol Gel Sci Technol.* 2008;45:63–72.
68. Provis JL, Palomo A, Shi C. Advances in understanding alkali-activated materials. *Cem Concr Res.* 2015;78:110–25.
69. Kumar S, Kumar R. Mechanical activation of fly ash: effect on reaction, structure and properties of resulting geopolymer. *Ceram Int.* 2011;37:533–41.
70. Ubbrìaco P, Bruno P, Traini A, Calabrese D. Fly ash reactivity. Formation of hydrate phases. *J Therm Anal Calorim.* 2001;66:293–305.
71. Panagiotopoulou Ch, Kontori E, Perraki Th, Kakali G. Dissolution of aluminosilicate minerals and by-products in alkaline media. *J Mater Sci.* 2007;42:2967–73.
72. Guimarães D, Oliveira VDA, Leão VA. Kinetic and thermal decomposition of ettringite synthesized from aqueous solutions. *J Therm Anal Calorim.* 2016;124:1679–89.
73. Fernández-Carrasco L, Vázquez E. Reactions of fly ash with calcium aluminate cement and calcium sulphate. *Fuel.* 2009;88:1533–8.
74. Sievert T, Wolter A, Singh NB. Hydration of anhydrite of gypsum ($\text{CaSO}_4 \cdot \text{II}$) in a ball mill. *Cem Concr Res.* 2005;35:623–30.
75. Hewlett PC, editor. *Lea's chemistry of cement and concrete.* 4th ed. London: Arnold; 1998.
76. Clark BA, Brown PW. The formation of calcium sulfoaluminate hydrate compounds. Part II. *Cem Concr Res.* 2000;30:233–40.
77. Brown PW, Bothe JV. The stability of ettringite. *Adv Cem Res.* 1993;5:47–63.
78. Taylor HFW. *Cement chemistry.* 2nd ed. London: Thomas Telford; 1997.
79. Shimada Y, Francis Young J. Thermal stability of ettringite in alkaline solutions at 80 °C. *Cem Concr Res.* 2004;34:2261–8.
80. Chindaprasirt P, De Silva P, Sagoe-Crentsil K, Hanjitsuwan S. Effect of SiO_2 and Al_2O_3 on the setting and hardening of high calcium fly ash-based geopolymer systems. *J Mater Sci.* 2012;47:4876–83.
81. Rattanasak U, Chindaprasirt P. Properties of alkali activated silica fume– $\text{Al}(\text{OH})_3$ –fluidized bed combustion fly ash composites. *Mater Struct.* 2015;48:531–40.
82. Kurdowski W. *Chemia cementu i betonu.* Kraków: Stowarzyszenie Producentów Cementu; 2010 (in Polish).
83. Kim Jong-Wan, Lee Hae-Geon. Thermal and carbothermic decomposition of Na_2CO_3 and Li_2CO_3 . *Metall Mater Trans B.* 2001;32B:17–24.
84. Lehman RL, Gentry JS, Glumac NG. Thermal stability of potassium carbonate near its melting point. *Thermochim Acta.* 1998;316:1–9.
85. El-Eswed BI, Yousef RI, Alshaaer M, Hamadneh I, Al-Gharabli SI, Khalili F. Stabilization/solidification of heavy metals in kaolin/zeolite based geopolymers. *Int J Miner Process.* 2015;137:34–42.
86. Shi C, Fernández-Jiménez A. Stabilization/solidification of hazardous and radioactive wastes with alkali-activated cements. *J Hazard Mater B.* 2006;137:1656–63.
87. Canfield GM, Eichler J, Griffith K, Hearn JD. The role of calcium in blended fly ash geopolymers. *J Mater Sci.* 2014;49:5922–33.

Publisher's Note Springer Nature remains neutral with regard to jurisdictional claims in published maps and institutional affiliations.